Quantifying Deformation in Gel Swelling: Experiments and Simulations

Evdokia C. Achilleos, Robert K. Prud'homme, and Ioannis G. Kevrekidis
Dept. of Chemical Engineering, Princeton University, Princeton, NJ 08544

Kostas N. Christodoulou
Avery Research Center, Pasadena, CA 91103

Kyle R. Gee
Molecular Probes Inc., Eugene, OR 97402

A technique for the real-time visualization of material line movement during transparent gel deformation was developed based on caged photo-activated fluorophores covalently attached to the gel network. It is used to quantitatively monitor the swelling of sodium polyacrylate and poly(acrylamide-sodium acrylate) gels in quasi two-dimensional constrained geometries. The experimentally obtained profiles for the Finger deformation tensor and the polymer concentration are compared with transient simulations of a model of transport in polyelectrolyte gels.

Introduction

Transient profiles for the concentration and deformation fields during swelling or shrinking is important in analyzing and designing processes that involve solvent transport in polymer networks; these arise in applications of polymer gels as, for example, superabsorbents (Buchholz and Peppas, 1994), drug delivery systems (Park, 1997), and artificial muscles (Shiga, 1997; Shahinpoor, 1996). Quantifying the deformation evolution during gel swelling and drying helps to understand the way material properties depend on process geometrical constraints and transient stress development. An experimental technique is applied here for real-time visualization of material line movement during polymer gel swelling. This technique was introduced recently by Achilleos et al. (2000a). The data obtained from polyelectrolyte gel swelling experiments is used to extract the polymer concentration and deformation profiles, which are compared with computational simulation results based on a transport model (Achilleos et al., 2000b).

One of the motivations for this work is to validate our computational transport model for the swelling and drying of polymer gels/films (Christodoulou et al., 1998; Powell et al., 1999b; Achilleos et al., 2000b). This model is based on multicomponent-multidimensional mixture theory (Powell et al., 1999a) which is an extension of the work of Lustig et al. (1992). It was first applied to two-component drying and swelling of nonionic films (Powell et al., 1999b). Two-component models for nonionic gels (Onuki, 1993; Durning and Morman, 1993; Doi and Onuki, 1992; Curtiss and Bird, 1996) are reviewed in Powell et al. (1999a, b). Other transient models, such as two-component models for small, isotropic deformations (Tanaka, 1978; Tanaka and Fillmore, 1979; Matsuo and Tanaka, 1988; Wang et al., 1997) based on the Tanaka-Hocker-Benedek theory (Tanaka et al., 1973), as well as phenomenological three-component models (Hariharan and Peppas, 1994; Grimshaw et al., 1990; Segalman and Witkowski, 1995), which may consider large-scale deformations, are discussed by Achilleos et al. (2000b). In that article the theory of Powell et al. (1999a) was extended to model polyelectrolyte gel swelling in salt solutions; extensive transient simulation data for the evolution of deformation, concentrations, and stress fields were obtained. Experimental data on the same fields can serve to validate the model.

Experimental data of gel swelling are mostly available in the form of overall mass uptake or shape measurements

Correspondence concerning this article should be addressed to I. G. Kevrekidis.

(Tanaka and Fillmore, 1979; Matsuo and Tanaka, 1988; Siegel et al., 1988; Firestone and Siegel, 1988; Sakohara et al., 1990; Dubroskii et al., 1989; Harmon et al., 1987; Scherer et al., 1991). Optical techniques, such as laser interferometry have been used to determine the velocity of the moving front in Case-II diffusion, along with the polymer weight fraction in the swollen layer (Durning et al., 1995). The diffusion coefficients of tagged macromolecules/particles in and out of a polymer gel have been measured through fluorescent measurements (Tong and Anderson, 1996; Dang and Saltzman, 1992; Haggerty et al., 1988).

Recently nuclear magnetic resonance (NMR) techniques have been applied to obtain solvent and polymer concentration profiles in polymer-solvent systems, and could potentially be used to obtain polymer deformation. One-dimensional (1-D) solvent concentration profiles for gel swelling were obtained for high polymer concentration regimes using an ^{1}H spin-echo NMR imaging technique (Hyde et al., 1995). A 1-D ^{1}H spin-echo NMR imaging technique with variable delay times decoupled the NMR signal intensities due to the polymer and the solvent, allowing for determination (at low polymer concentration regimes) of concentration profiles for both (Hyde and Gladden, 1998). NMR has also been used to study 2-D swelling and water mobility in initially glassy polymers (Kojima et al., 1998); transverse and coronal section images of swelling tablets provide information on the moving hydration front, but not the concentration profile (c.f. (Hyde and Gladden, 1998)). NMR-based grid writing techniques (Kutter et al., 1998; Moser et al., 1999) have been used to measure fluid velocity profiles but have not yet been modified to apply to the slow motions associated with gel swelling.

The PHoto Activated Nonintrusive Tracking of Molecular Motion (PHANTOMM) gel swelling technique introduced by Achilleos et al. (2000a) allows for spatially resolved measurements of both polymer concentration and deformation tensor components, in 1-D and 2-D, by monitoring the movement of permanently tagged material lines. It originated from a flow velocimetry technique PHANTOMM (Lempert et al., 1994, 1995). Photo-activated fluorophores (PAFs) are potentially fluorescent compounds which have been covalently bonded to a caging group that quenches fluorescence, for example, di-methoxy-nitrobenzyl caged fluorescein (Lempert et al., 1995). This caging group can be cleaved by shining a UV laser beam through the transparent material, releasing the fluorescent compound. In PHANTOMM, a trace concentration of PAFs is dissolved in the flow liquid and a UV laser beam is used to ''write'' a line in the flow by uncaging the fluorophore. This line fluoresces when illuminated by a light source, and velocity measurements are made by visualization of its temporal displacement. The technique presented here is based on copolymerizing a PAF, which is attached on a monomer, with the gel network. When the fluorophore is uncaged (using a laser beam) a line, permanently anchored on the gel, is written. Material grids are thus written and their movement is continuously monitored during gel deformation.

A description of the experimental techniques is given. The model and simulations are briefly presented. In the results section raw and processed experimental data are presented and compared with model predictions, followed by a discussion section.

Experimental Studies

Gel synthesis

Two types of gels, sodium polyacrylate and poly(acrylamide-sodium acrylate), were copolymerized with the dye-tagged monomer. Water-soluble caged fluorescein, 5-carboxymethoxy-2-nitrobenzyl-caged fluorescein-5-acrylamide (bis-CMNB-caged fluoresceinacrylamide), shown in Figure 1, was used as the dye. It was synthesized by adapting the caged fluorescein chemistry (Mitchinson et al., 1998): a polymerizable caged fluorescein was produced by the acylation (with acryloyl chloride) of 5-aminofluorescein, caged with two water-solubilizing CMNB (sodium salt) groups. Absorbance and fluorescence spectra of sample dye solutions used in this experiment are similar to the ones in Lempert et al. (1995). The caged dye absorbs light at 320 nm, and an extinction coefficient of 12×10^6 cm^2/mol can be used to determine the exact dye concentration in solution. The completely uncaged dye (5-acrylamido-fluorescein) has an extinction coefficient of 8×10^6 cm^2/mol. Absorbance spectra with peaks at 488 nm and 440 nm indicate the presence of uncaged and monocaged dye, respectively. The fact that the fluorophore spontaneously uncages at high temperatures, and at extreme pH (pH <1, pH >10), was taken into account during gel preparation. The gels were prepared so that the pH after gelation would be above 7 to maximize fluorescence (Haugland, 1996).

For the sodium polyacrylate gels, a polymerization and gelation protocol for polyacrylic acid gels (Yin et al., 1992; Mandigo, 1998) was modified to allow for the dye copolymerization. We prepared gels with 15.2 wt % concentration of 80% neutralized acrylic acid, 1.2 mol % cross-linker (/monomer) density, and 7 mg/L dye concentration.

The solution was sparged to remove oxygen for one hour by purging with nitrogen under vacuum; vacuum was then

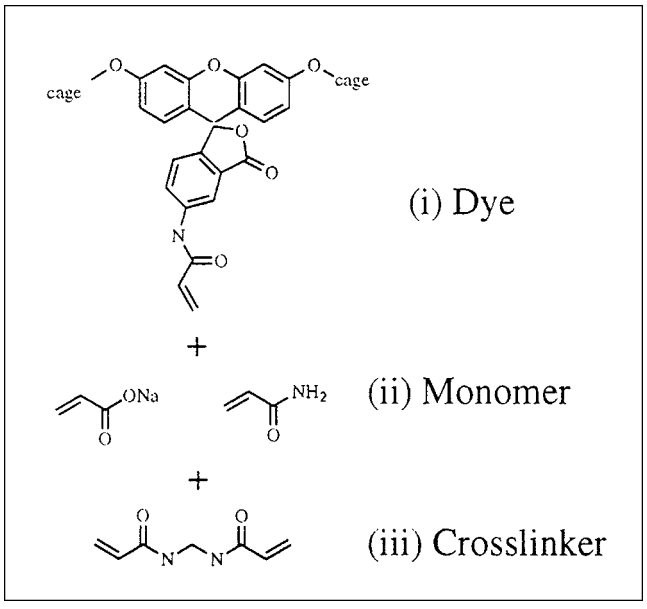

Figure 1. Gel chemistry.

The dye used was 5-carboxymethoxy-2-nitrobenzyl-caged fluorescein-5-acrylamide, the monomers were sodium acrylate and acrylamide, and the cross-linker was bisacrylamide.

broken, and the initiators, 200 μL ascorbic acid solution (0.155 g in 10 mL) and 400 μL sodium persulfate solution (0.755 g in 10 mL) were added. The solution was degassed for 5 more min before transferring to the molds. All mixing and degassing steps were performed in an ice/water bath. Spontaneous uncaging of the dye during the polymerization caused background fluorescence in the gel. The polymerization temperature was set to 60°C for 2 h instead of 80°C for 1 h, as in Yin et al. (1992) and Mandigo (1998), because the dye uncages faster at high temperatures and the amount of persulfate was increased to 0.036 wt % to compensate for the temperature reduction. The gels were left for 24 h at room temperature and then refrigerated. The degree of neutralization of the acrylic acid was chosen so that the pH after gelation was above 7, based on the measurements in Yin (1993). Higher degrees of neutralization result in more fluorescence (through higher gel pH), but also in lower cross-linking efficiency (Yin, 1993; Anseth et al., 1996). The dye-tagged monomer does not polymerize with the same efficiency as the acrylic acid; a significant percentage of dye thus is not chemically attached to the gel. The lower reactivity of the dye could be due to steric hindrance and the relative intensity of the fluorescent beam before and after unattached dye diffuses away could be used to estimate the percentage of dye cross-linked to the polymer.

For the poly(acrylamide-sodium acrylate) copolymer, a polymerization protocol by Biorad (1999) was used. For these gels, the degree of gel ionization could be chosen independently of the pH. Gels with 13.252 wt % (overall) polymer concentration at 20% ionization (that is, 20% of monomers were sodium acrylate, and the remainder were acrylamide), 0.327 mol % cross-linker (/monomer) density, and 7 mg/L dye concentration were prepared. The pre-gel solution was degassed for 12 min at ambient temperature. The initiators, 0.2 mL of 10 wt % ammonium persulfate (Sigma) and 0.04 mL of TEMED (Sigma), were added to the solution, which was then transferred to the molds and placed at a 21°C water bath. Visible gelation started about 20 min after initiator addition, and the gelation was complete after 2 h. Again, the gels were refrigerated after being at room temperature for 24 h. When initiators are added to the gel solution, the pH increases rapidly to pH $\simeq$ 10, and then decreases to a final value of 8.7. More uncaging during polymerization was observed in these gels, but the dye copolymerized more efficiently. Since the monomer attached to the dye is acrylamide, it is reasonable that the dye copolymerizes more efficiently in the conditions best suited for acrylamide gels (rather than the conditions best suited for sodium acrylates). The solution pH before and during polymerization is expected to greatly affect the efficiency of the dye copolymerization.

The uncaging in these gels can be attributed to the initial pH and temperature rise (exothermic reaction), but also possibly to the attack by free radicals from the polymerization initiator. As explained in Biorad (1999) it is important for the pH to be above 7 for gelation to take place. There is still room for experimentation in order to achieve less uncaging during polymerization of the poly(acrylamide-sodium acrylate) gels. This could be achieved by further reduction of the initial gel pH or the amount of initiator added.

The molds used in the polymerization were rectangular (4.4$\times$1$\times$1 cm) quartz cuvettes, which were surface treated. They were first cleaned in a two-step acid/base treatment (Decher et al., 1992; Decher and Hong, 1991), which resulted in hydrophilic surfaces. They were then hydrophobically coated with dimethyl-dichloro-silane solution (5% in heptane-Fluka Gel Repel I) with four repetitive coats, each followed by 15 min heating at 130°, rinsing with deionized water, and drying (Beck, 1998). In order to enforce the attachment of the gel on a rigid substrate, as will be discussed later, a piece of filter paper (4.35$\times$0.98$\times$0.05 cm) was embedded in the gel by placing it inside the cuvette, on one wall, prior to the introduction of the gel solution.

Laser reading/writing apparatus

A Q-switched Nd-YAG laser beam (third harmonic, 355 nm (Lempert et al., 1994, 1995)) was used to uncage the dye (write lines), while the gel was in the quartz cuvette as shown in Figure 2. Using a motorized vertical translator (Oriel motor mike model No. 16627) attached to a remote controller (Oriel motor mike controller model No. 18006), a 10$\times$10 grid of lines, 1 mm apart and approximately 0.1 mm thick, was written on the 1$\times$1 cm^2 cross-sectional area of the gel. The absorbency of the dye at 355 nm is due only to the caging groups and, provided that the laser energy is high enough to uncage all dye in its path, the fluorescence lines are homogeneous along the 1 cm path; this was qualitatively observed in the experiments. The thickness of the lines is determined by the number and energy of the pulses used to write the grid; this also affects the visual contrast between written lines and background fluorescence due to dye that was uncaged during polymerization, as well as uncross-linked, laser-uncaged dye, which then diffuses away from the grid. Good contrast is important for accurately monitoring material line movement. An initial dye concentration of 7 mg/L in the gel and 7–10 pulses of 0.6 mJ per pulse for each of the lines written was an effective combination for good contrast.

A thin needle was inserted in a corner of the cuvette and a small amount of water was injected in order to force the gel

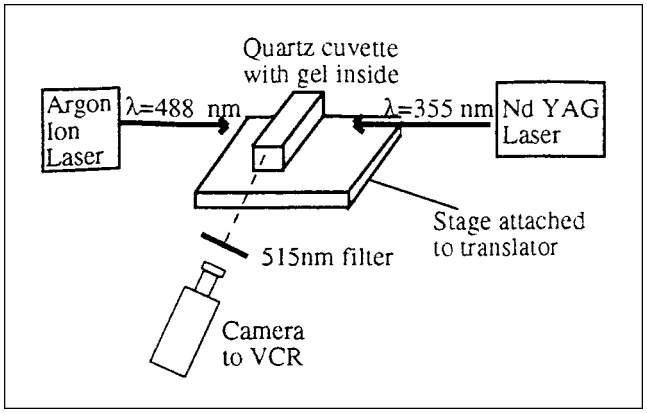

Figure 2. Experimental setup for line writing through the cross-section of the polymer gel.

The quartz cuvette containing the gel was placed on a stage translator. The Nd YAG laser was used for line writing, the argon ion laser was used for interrogation of the written lines, and the camera for viewing the writing of the lines.

from the mold after the grid was written; a 6 mm-thin slab whose center contains the grid was then sliced. Experiments for two different swelling geometries were then performed. In both geometries shown in Figures 3b and 3c the gel slice was sandwiched between two hydrophobically coated glass plates which were surface-treated following the same procedure as in the treatment of the molds. This prevented swelling in the third dimension. Furthermore, by writing lines perpendicular to the plates (along the third, thin dimension of the gel slice, z) and observing their parallel displacement during swelling, we confirmed that the hydrophobically coated plates behaved as a no-shear boundary. This ensured the two-dimensionality of the swelling.

The first geometry was a gel slab, attached to a rigid substrate, free to swell in the x and y directions, and sliding along a boundary wall in the z direction, as shown in Figure 3b. In order to attach the gel on the substrate, the bottom of the gel slice (the side in which the filter paper was introduced) was glued on a polystyrene mounting shim ($\delta = 0.24$ mm) with cyanoacrylate (Loctite 401) and RTV silicon rubber (General Electric) was used to glue the shim on the Plexiglas base plate. The filter paper was used in order to constrain the gel by attaching it to the rigid substrate; as the gel swells the filter paper acts as part of the network (Figure 3b). The second geometry was one of a gel disk, swelling again in the $x - y$ plane, but additionally confined between two rigid planes at $y = 0$ and $y = 0.8$ cm, as shown in Figure 3. This was motivated by our eventual interest in examining how an array of particles would swell against each other. This gel disk was not glued on any of the plates, yet it did not move in the horizontal direction; it was held in place by friction. The swelling cells in each case were placed in a 1.5 L glass tank as shown in Figure 3a.

A thin sheet of $\lambda = 488$ nm light from an Argon ion laser was used to interrogate the grid, which fluoresced with emission maximum at 520 nm. Grid fluorescence during the experiment was monitored through a CCD camera (Cohu model 4910 S) connected to a VCR. Solvent (NaCl aqueous solution) is poured in the tank to initiate swelling (Figure 3a); the experiments last several (up to 40) h. Photobleaching did not occur to a significant extent, because the gels were interrogated only when data were being collected. Furthermore, the interrogation intensity was not high (as would be in the case of confocal microscopy). The intensity of the grids was, however, partially reduced during the experiments due to dye dilution with swelling.

Images were digitized using a Power Macintosh with a Scion LG-3 frame grabber and NIH imaging software; averaging

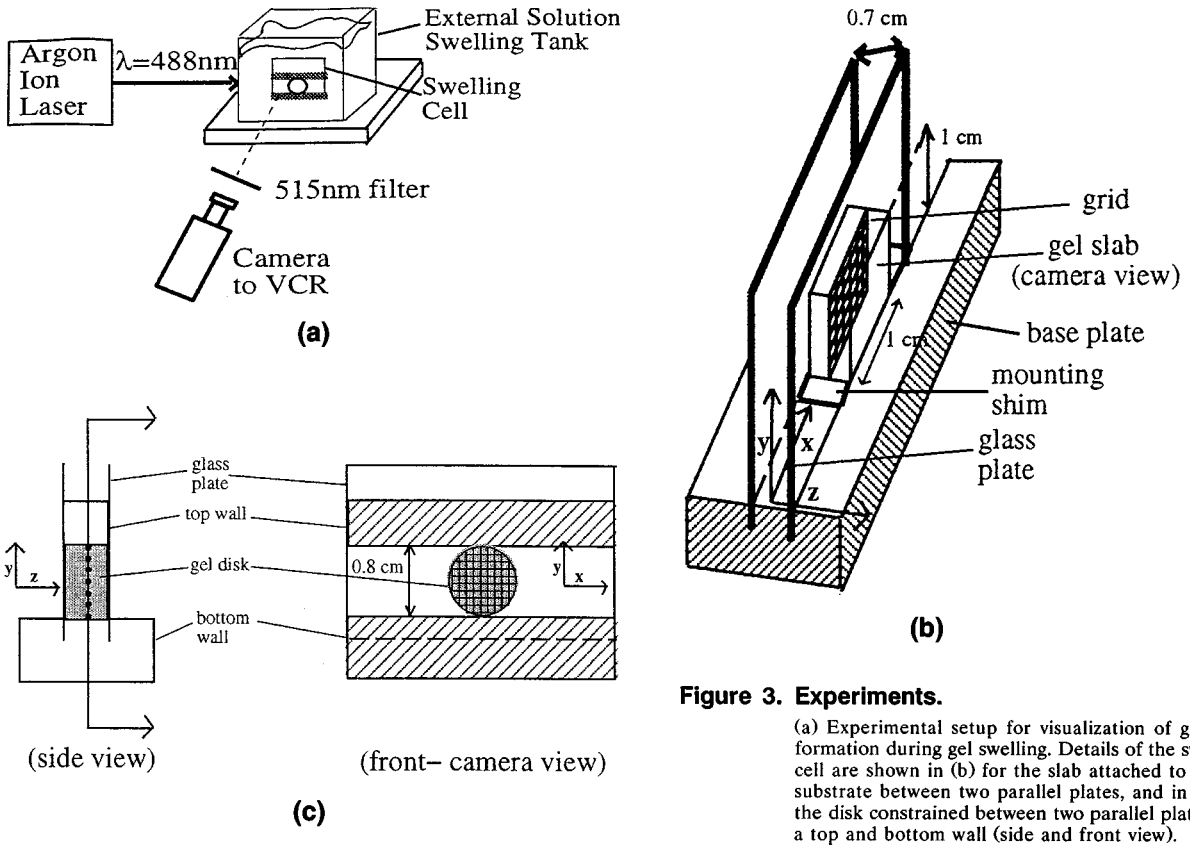

Figure 3. Experiments.

(a) Experimental setup for visualization of grid deformation during gel swelling. Details of the swelling cell are shown in (b) for the slab attached to a rigid substrate between two parallel plates, and in (c) for the disk constrained between two parallel plates and a top and bottom wall (side and front view).

over 25 frames (1 s) greatly improved image quality and grid/background contrast.

Polyelectrolyte Gel Transport Model: Thermodynamics and Kinetics

A transport model developed by extending the multicomponent-multidimensional theory of Powell et al. (1991a) to polyelectrolyte mixtures (Achilleos et al., 2000b) was used to simulate swelling of the gel slab attached to a rigid substrate (Figure 3b) in a salt solution. The model is accurate for low degrees of ionization and thus appropriate for the poly(acrylamide-sodium acrylate) gel. The model equations are briefly summarized here, nondimensionalized with the characteristic quantities in Table 1. Boldface small letters represent vectors and boldface capital letters represent tensors.

Under the assumptions of negligible inertia, constant-equal partial species densities, and electroneutrality, the conservation laws for species mass, polymer mass, overall momentum, and overall charge for a mixture of 4 components ($\alpha \equiv 1$ to 4, $1 \equiv H_2O$, $2 \equiv Na^+$, $3 \equiv Cl^-$, $4 \equiv p$ the polymer) are

$$\rho \frac{d_p w_\alpha}{dt} - \rho \frac{w_\alpha}{w_p} \frac{d_p w_p}{dt} + \nabla \cdot \left(j_\alpha - \frac{w_\alpha}{w_p} j_p \right) = 0 \tag{1}$$

$$\nabla \cdot \boldsymbol{v}_p + \frac{1}{\rho} \frac{d_p \rho}{dt} + \frac{1}{w_4} \frac{d_p w_p}{dt} = 0 \tag{2}$$

$$\nabla \cdot \boldsymbol{\sigma}_p - \nabla P = 0 \tag{3}$$

$$\sum_{\alpha=1}^{p} z_\alpha w_\alpha \frac{M_1}{M_\alpha} = 0. \tag{4}$$

Here ρ, $\boldsymbol{v}_p$, $\boldsymbol{\sigma}_p$, and P are the mixture density, polymer velocity, network stress, and hydrostatic pressure; w_α, j_α, M_α, and z_α are the species (α) weight fraction, diffusive flux, molecular weight and charge respectively and d_p/dt is the substantial derivative following the polymer velocity. As discussed in Powell et al. (1999a, b), the pressure in these equations is indeterminate as in compressible fluid mechanics. The diffusive flux of components α is

$$j_\alpha = -\overline{D}_\alpha w_\alpha \left(\nabla \pi_\alpha + \frac{M_\alpha}{M_1} \nabla \cdot \sigma_p + z_\alpha \nabla \mathcal{E} \right) \tag{5}$$

where π_α and $\overline{D}_\alpha$ are the osmotic pressure and diffusion coefficient of component α and $\mathcal{E}$ is the electrical potential. The free energy of the mixture can be used to obtain the network stress and the osmotic pressure. The free energy consists of mixing, elastic, and electrostatic contributions (Achilleos et al., 2000b). Multicomponent Flory-Huggins (FH) mixing (Flory, 1953), affine network rubber elasticity (Hermans, 1962), and additive charging of the free ions (Fowler and Guggenheim, 1965) and of rod-like polymer chains (Stigter, 1975; Manning, 1969) were combined (Achilleos et al., 2000b). The osmotic pressure of each component is related to its chemical potential μ_α and the hydrostatic pressure P through $\mu_\alpha = \pi_\alpha + (M_\alpha/M_1)P$. The osmotic pressure ($\pi_\alpha$) of the free components (1 to 3) was derived from the free energy expression

$$\pi_\alpha = \left(\ln w_\alpha + \chi_{\alpha p} w_p + 1 \right) - w_p \sum_{\beta=1}^{p-1} \frac{\chi_{\beta p} w_\beta M_\alpha}{M_\beta} - \sum_{\beta=1}^{p-1} \frac{w_\beta M_\alpha}{M_\beta} + C_{DH} \left(I_s^{1.5} \frac{M_\alpha}{M_1} - 3 z_\alpha I_s^{0.5} \right) + C_{mf} a^2 w_p \left(- \frac{z_\alpha^2 M_1}{I_s M_\alpha} + 1 \right) \tag{6}$$

where $\chi_{\alpha p}$ is the FH interaction parameter of component α with the polymer. The interaction parameter of water and polymer was taken to be the one of water and uncharged polymer ($\chi_{1p} = 0.5$), and the ones of ions and polymer were neglected ($\chi_{2p} = \chi_{3p} = 0$) since the electrostatic interactions dominate. The degree of gel ionization is given by a, and the dimensionless ionic strength of the mixture is given by $I_s = \sum_{i=1}^{p-1} [(w_i M_1/M_i) z_i^2]$, where the constants C_{DH} and C_{mf} are 2.06 and 0.33, respectively (Achilleos et al., 2000b). The network stress $\boldsymbol{\sigma}_p$ is

$$\boldsymbol{\sigma}_p = G_0 \frac{\phi_p}{\phi_{p0}} (\mathbf{B} - \mathbf{I}) \tag{7}$$

where G_0 and w_{p0} are the gel modulus and polymer weight fraction at gelation, and $\boldsymbol{B}$ is the Finger deformation tensor. Using an identity for the effective conformation tensor ($\boldsymbol{B} - \boldsymbol{I}$) as in Edwards and Beris (1990), the following rate expression can be used to relate the network stress to the polymer velocity ($\boldsymbol{v}_p$), and d_p/dt

$$\overset{\square}{\boldsymbol{\sigma}}_p \equiv \frac{d_p \boldsymbol{\sigma}_p}{dt} - \boldsymbol{\sigma}_p \cdot \nabla \boldsymbol{v}_p - \nabla \boldsymbol{v}_p^T \cdot \boldsymbol{\sigma}_p + \boldsymbol{\sigma}_p \nabla \cdot \boldsymbol{v}_p = G_0 \frac{\Phi_p}{\Phi_{p0}} \left(\nabla \boldsymbol{v}_p + \nabla \boldsymbol{v}_p^T \right). \tag{8}$$

Equations 1–6 and 8 were solved numerically with a finite-element code developed by Christodoulou and cowork-

Table 1. Characteristic Quantities for Nondimensionalization

Variable	*Characteristic Quantity*	
x, y	L_0	initial gel thickness, 1 cm
ρ, ρ_α	ρ_0	$= \rho_w$, water density, 1 g/cm^3
$\overline{D}_\alpha$	D_0	= water diff. coeff. at the beginning of swelling, 7.46×10^{-4} cm^2/s
t	t_0	$= L_0^2/D_0$ 24 min
v, v_α	v_0	$= D_0/L_0 = L_0/t_0$, 0.042 cm/min
π_α	$R\Theta d_\alpha/M_\alpha$	2478.65 J/mol d$_\alpha$/m$_\alpha$
μ_α	$R\Theta$	2478.65 J/mol
σ_p, P, G_0	$R\Theta d_1/M_1$	137.7 MPa
j_α	j_0	$= \rho_0 v_0$, 0.042 g/(cm·min)
$\mathcal{E}$	$\mathcal{E}_0$	$= R\Theta/\mathcal{F}$, 0.2469 V

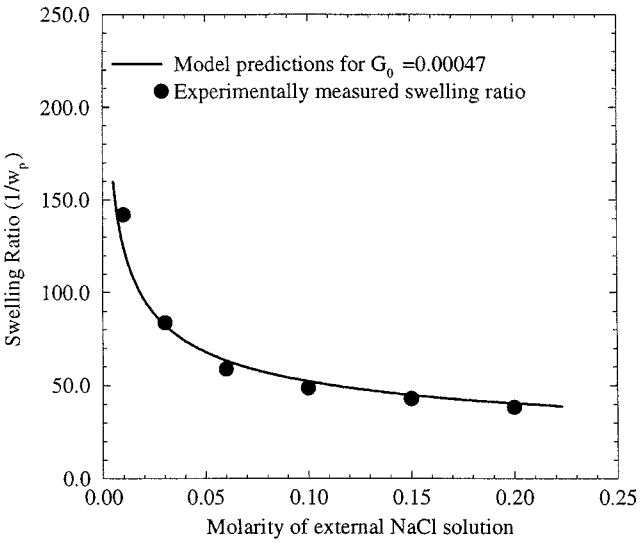

Figure 4. Modulus determination for poly(acrylamide-sodium acrylate) gel with $a = 0.2$.

Experimentally measured swelling ratios and model predictions for $G_0 = 0.00047$.

ers (Christodoulou and Scriven, 1992; Christodoulou et al., 1998; Christodoulou, 1990; Powell et al., 1999b) as described in Achilleos et al. (2000b). The boundary conditions for the network stress and the diffusive flux at the free interface are

$$n\cdot\left(\sigma_p^g - P^g I\right) = P^{\text{ext}} \tag{9}$$

$$j_\alpha = n\cdot(\boldsymbol{v}_a - \boldsymbol{v}_I) = Sh\left(\mu_\alpha^g + z_\alpha \mathcal{E}^g - \mu_a^{\text{ext}} - z_\alpha \mathcal{E}^{\text{ext}}\right) \tag{10}$$

where n is the normal vector to the interface, $\boldsymbol{v}_I$ is the velocity of the interface, and Sh is the Sherwood number $\equiv kL_0/D_o$. A time-dependent $Sh = 10{,}000 \tanh(20\,t)$; that is, a smooth, rapid increase of the mass-transfer coefficient (k) to a practically infinite value was used to model the initial contact of the gel with the external liquid solution. The initial modulus $G_0 = 0.00047$ ($= 64.67$ kPa) of the poly(acrylamide-sodium acrylate) copolymer gels was determined by fitting the equilibrium predictions of the model for isotropic gel swelling in NaCl solutions with molarities ranging from 0.01 M to 0.2 M NaCl, as shown in Figure 4.

The water diffusion coefficient (D_1) was obtained from the friction coefficient (f) measurements of water in acrylamide gels by Tokita (1993)

$$D_1 = \frac{d_1}{M_1 R\Theta}\frac{(1-w_1)}{f}. \tag{11}$$

For the gels with $w_{p0} = 0.12467$ (not including the dissociated counterions) and cross-linker density $C = 0.327$ mol %, D_0, the initial water diffusion coefficient, was determined from the experimental data in Tokita (1993) to be 7.4610^{-4} cm^2/s. The dependence of the friction factor coefficient on polymer weight fraction in the data of Tokita (1993) was fitted by Tong

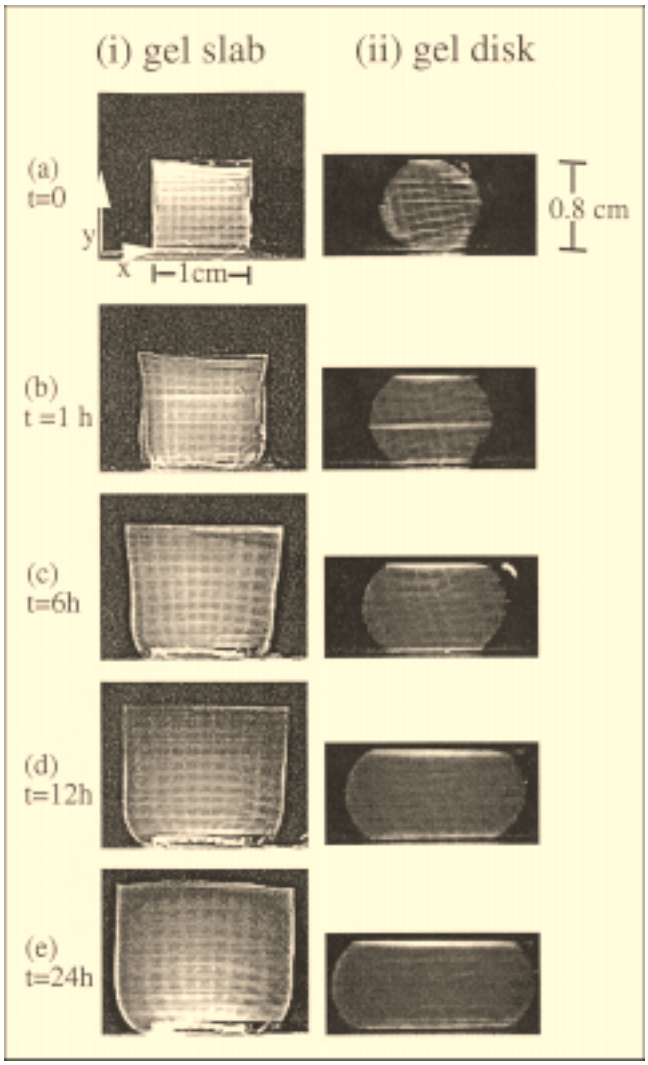

Figure 5. Swelling of poly(acrylamide-sodium acrylate) gel in 0.1 M NaCl solution with simultaneous visualization of a material grid for the slab geometry in (i) and the disk geometry in (ii).

The snapshots were recorded at (a) $t = 0$, (b) $t = 1$ h, (c) $t = 6$ h, (d) $t = 12$ h, and (e) $t = 24$ h.

(1995) to be

$$f = f_0\left(\frac{w_p}{w_{p0}}\right)^{1.42}. \tag{12}$$

Since the ions were at infinite dilution, their diffusion coefficients were determined from their ionic mobilities (u_α) (Cussler, 1994)

$$D_\alpha = u_\alpha R\Theta; \tag{13}$$

At room temperature, $D_2 = 1.33\times10^{-5}$ cm^2/s and $D_3 = 2.03\times10^{-5}$ cm^2/s were used for Na^+ and Cl^-, respectively.

Results

A sequence of processed images obtained for poly(acrylamide-sodium acrylate) gels swelling in 0.1 M NaCl solution is

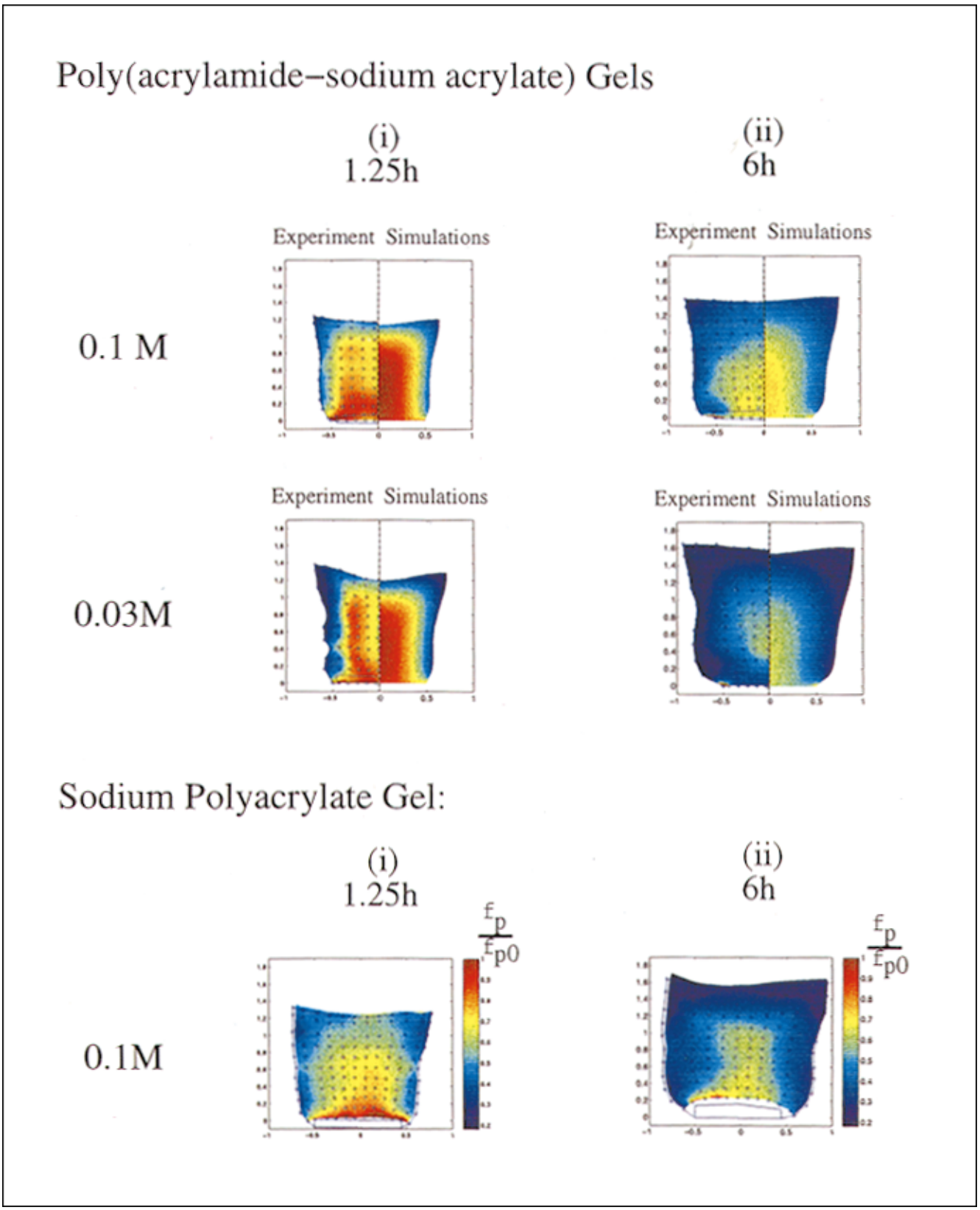

Figure 6. Swollen polymer concentration field (scaled by the initial concentration) field after (i) $t = 1.25$ h and (ii) $t = 6$ h.

Open circles represent nodal positions and the solid line represents the perimeter of the gel. Sodium polyacrylate gel swelling in 0.1 M NaCl solution shown in (a), and poly(acrylamide-sodium acrylate) gel swelling in 0.1 M, and 0.03 M shown in (b) and (c), respectively. In (b) and (c): left experiment; right simulations.

shown for the gel slab and disk geometries in Figure 5 in the i and the ii, respectively. Sample images of the fluorescent material grid are shown at six swelling times, with the first one (Figure 5a) taken immediately after the initiation of swelling and the last one (Figure 5e) being very close to equilibrium. The material coordinates (X) of the grid nodal positions (tabulated from line intersection points) are taken at the beginning of swelling, when the gel is stress-free (Figure 5a). Nodal positions at later times are the spatial coordinates (x) (in Figures 5b–5e); the Finger deformation tensor B (Macosko, 1994) is thus obtained

$$B = \left(\frac{\partial x}{\partial X}\right) \cdot \left(\frac{\partial x}{\partial X}\right)^T \tag{14}$$

where $x_1 = x$, $x_2 = y$, and $x_3 = z$ in our coordinate system. The components of B can be used to obtain several physical quantities either directly or through a constitutive law. For example, the determinant of B, III_B, can be used to relate the polymer concentration ϕ_p to the initial one (ϕ_{p0})

$$\phi_p(X, t) = \phi_{p0}\, III_B^{-1/2} \tag{15}$$

In Figure 6, the scaled polymer volume fraction (ϕ_p/ϕ_{p0}) is plotted for different gel slab experiments. The intersections of the grid with the gel surface provide the outermost nodal positions; the thin layer of gel below the filter paper (on the side attached to the rigid substrate) causes a slight distortion of the filter paper during swelling. This slight distortion (and its shadow) is clearly seen in the i section of Figure 5. The boxed space in Figure 6 represents the area occupied by the filter paper. Results at two different times: 1.25 h and 6 h after the start of swelling are shown in sections i and ii of Figure 6. Polymer volume fractions are plotted for the sodium polyacrylate gel swelling in 0.1 M solution in (a), and the poly(acrylamide-sodium acrylate) swelling in 0.1 M and 0.03 M solutions in (b) and (c), respectively. For the sodium polyacrylate gels, the experimentally determined profiles (left) are compared with the ones obtained from the numerical simulations as described in the previous section. For all parameters, the polymer concentration as expected decreases as swelling proceeds from 1.25 h to 6 h. The polymer volume fraction is higher at the interior of the gel, especially close to the bottom, where the gel is attached to the substrate. The sodium acrylate gel, with a higher degree of ionization as well as higher initial volume fraction, swells more than the poly(acrylamide-sodium acrylate) gel in the 0.1 M solution. As expected, the gel in the 0.03 M solution swells much more than the one in the 0.1 M solution. As discussed in Achilleos et al. (2000b), the transient, and, in this case of constrained swelling, also the final gel shape, depends on the polymer concentration and stress profiles. Lower polymer concentration near the free edge, especially in the case of higher swelling, leads to higher water diffusion coefficient and lower modulus. In addition to this, the diffusion near the free edge is 2-D as opposed to the diffusion near the symmetry line which is 1-D; this leads to higher stresses and less swelling near the center. These factors and thus the irregularity in the gel shape are intensified when the overall swelling is higher, as can be seen when comparing Figure 6b and c. For all these features and at both swelling times, good agreement is observed between simulations and experimental data, not just qualitatively, but also quantitatively.

The components of the Finger deformation tensor are presented in Figure 7 for the sodium acrylate gel swelling in 0.1 M NaCl solution. These are compared with the simulation results for gel swelling at 1.25 h in (i), and 6 h in (ii). The B_{xx} extensional deformation is, as expected, larger at the two sides of the gel. This feature is more intense at the beginning of swelling (1.25 h); B_{xx} increases and becomes more uniform as swelling proceeds (6 h). Similarly, the B_{yy} extensional deformation is larger at the top of the gel and that too increases and becomes more uniform as the swelling proceeds. Again, good agreement is observed for these features between model and simulations: B_{xx} and B_{yy} can be essentially quantitatively predicted computationally from the simulations. Assuming that the intersection of the written lines can be found within an error equal to 10% of the line thickness, the expected error, due to experimental measurement, in B_{xx} and B_{yy} was calculated to be 3% when B_{xx} is approximately 1 and 5% when it is approximately 3. The deviation of the simulation results from the experimental measurements in Figures 5 and 6 is at most 10%. The geometry of this experiment gives rise to anisotropic deformation and stresses, making the shear deformation B_{xy} nonzero. In Figure 7c B_{xy} is shown at the two swelling times. This component of the deformation tensor is much smaller than the extensional ones. In the experiment B_{xy} is maximum right at the free corner, whereas in the simulations this local maximum lies slightly inside the gel. B_{xy} increases at the curved surface near the bottom of the gel and approaches 0 at the middle of the top side (again in agreement with simulations) since the top middle essentially undergoes unconstrained 2-D swelling. Even though the agreement for this shear component of **B** is not quite quantitative, the development of shear deformation is reasonably captured. In Figure 8, the extensional deformation of the gel swelling for 6 h in NaCl solutions of 0.1 M and 0.03 M is shown. Clearly, the gel swells more in the 0.03 M solution, as reflected from the large values of B_{xx} and B_{yy}. The predicted values for these components of **B** are in quantitative agreement with the simulations for both external solution molarities.

Summary and Conclusions

A technique for visualizing dynamic deformation of gels during swelling was presented. Spatially resolved polymer concentration and deformation fields were obtained for gel swelling in two different geometries, and for the first time compared to simulation profiles obtained with the model of Achilleos et al. (2000b). Measurements and predictions of ϕ_p, B_{xx}, B_{yy}, and B_{xy} were made and found to be in agreement with the model. To our knowledge, this is the first time that 2-D fields of polymer deformation in gel swelling were experimentally measured and compared with simulation predictions. Modeling the constrained disk geometry by implementing a penalty term to enforce the constraining boundaries (top and bottom plate) is currently under way. The technique used here could also be used in other gel processes including drying and shaping to determine the polymer concentration and deformation profiles. Through an appropriate stress law, σ_{xx}, σ_{yy}, and σ_{xy} can be obtained from B_{xx}, B_{xy}, and B_{yy}, for example, in an affine-network rubber elasticity model (Smith

et al., 1964)

$$\boldsymbol{\sigma}_p = G_0 \frac{\phi_p}{\phi_0}(B - I). \tag{16}$$

Being able to measure the transient deformation profiles in this way is important for validation of any transport model. A valid transport model is vital in many gel applications and geometries, especially in cases where the transient values of deformations and stresses overshoot their equilibrium value.

This technique has a time resolution limited only by camera frame rates and can be used to obtain spatially resolved concentration and deformation profiles. When continuous interrogation is used (as in the experiments presented here), pictures can be obtained at the standard video framing period (16.67 ms) (Lempert et al., 1995). Use of pulsed interrogation, as in Lempert et al. (1995) and Biage et al. (1996), would allow for multiple images to be obtained in one frame (that is, one image every 1 m·s). There is no limitation on the polymer or solvent concentrations, as long as the gel re-

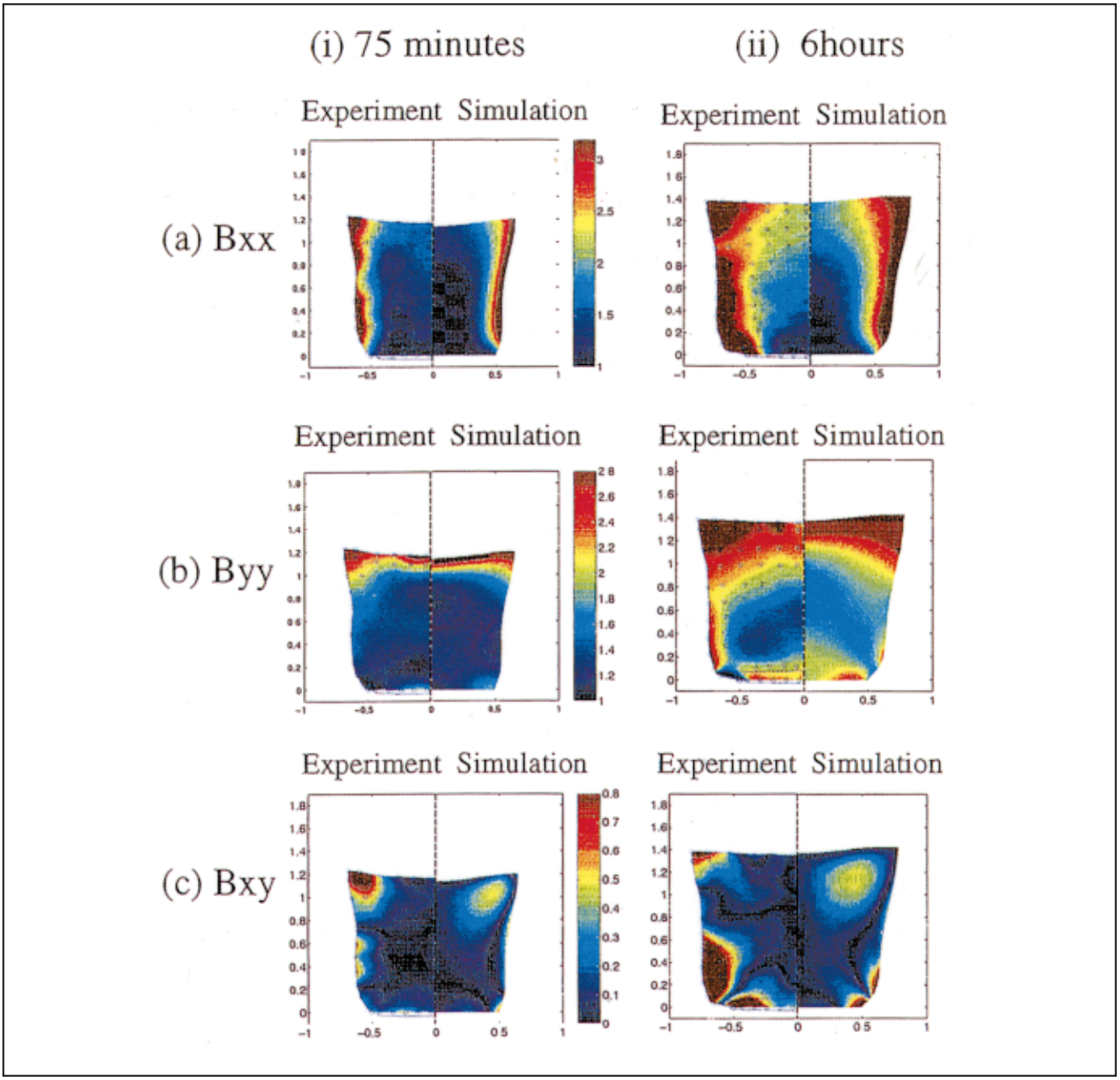

Figure 7. Finger deformation tensor components of the poly(acrylamide-sodium acrylate) gel at 1.25 h in (i), and 6 h in (ii).

Extensional components B_{xx} and B_{yy} are shown in (a) and (b), respectively, and the shear component B_{xy} is shown in (c). Left experiment; right simulation.

mains transparent and a fluorescent dye appropriate for the pH regime of the experiment is used. The technique can be directly extended to 3-D geometries. Using an optical microscope assembly as in Ishihara et al. (1997), the resolution can be improved on; thinner lines (5–10 μm thin) can be written every 50–100 μm, for example. Taking advantage of the fact that this dye has two caging groups, a two-photon uncaging technique, as in Pettit et al. (1997), could be used to essentially write ''points'' by writing short lines, 3 μm thick and 10 μm long. While no other technique has been used to measure deformation profiles in polymer gels, spin-echo NMR techniques provide polymer concentration profiles (Hyde and Gladden, 1998). However, in the low polymer concentration regime, the resolution in terms of the polymer volume fraction is low. The NMR velocimetry technique developed by Kutter et al. (1998) and Moser et al. (1999) would be a more appropriate one for measuring deformation. In this technique a material grid was written in water flow for different geometries from which the velocity and deformation of water could be obtained. A material line can however only be tagged for times smaller than the longitudinal NMR relaxation time T_1 (3 s for pure water and smaller in a polymer solution or gel (Hyde and Gladden, 1998)). Our technique is therefore better suited for slow swelling experiments.

Further work on optimizing certain quantitative features of the technique in order to improve contrast in the visualization of the material lines is under way. This would facilitate automatic data reduction methods as an alternative to manual tabulation of nodal positions for these data sets. A stochastic algorithm for determining edges (such as the ''crazy climber'' algorithm) or following lines (''snakes'') (Carmona et al., 1998) can be used to reconstruct fine lines whose intersections can be automatically tabulated. Professor R. Carmona (CE/OR at Princeton) and his group have started examining how these algorithms should be altered in order to perform such tasks on our data.

We believe that through direct observations, as well as validation of predictive models, this technique can play an important role in understanding transport and stress development in polymer processing applications.

Acknowledgments

We are grateful to W. R. Lempert for helping start our experiments, and to S. R. Harris, M. Beck, R. B. Miles, S. Suckewer, and S. M. Troian for help with the experimental setup/equipment usage. This work was partially supported by the National Science Foundation, in part through the NPACI San Diego supercomputing center; all our computations were performed on the Cray T90 there.

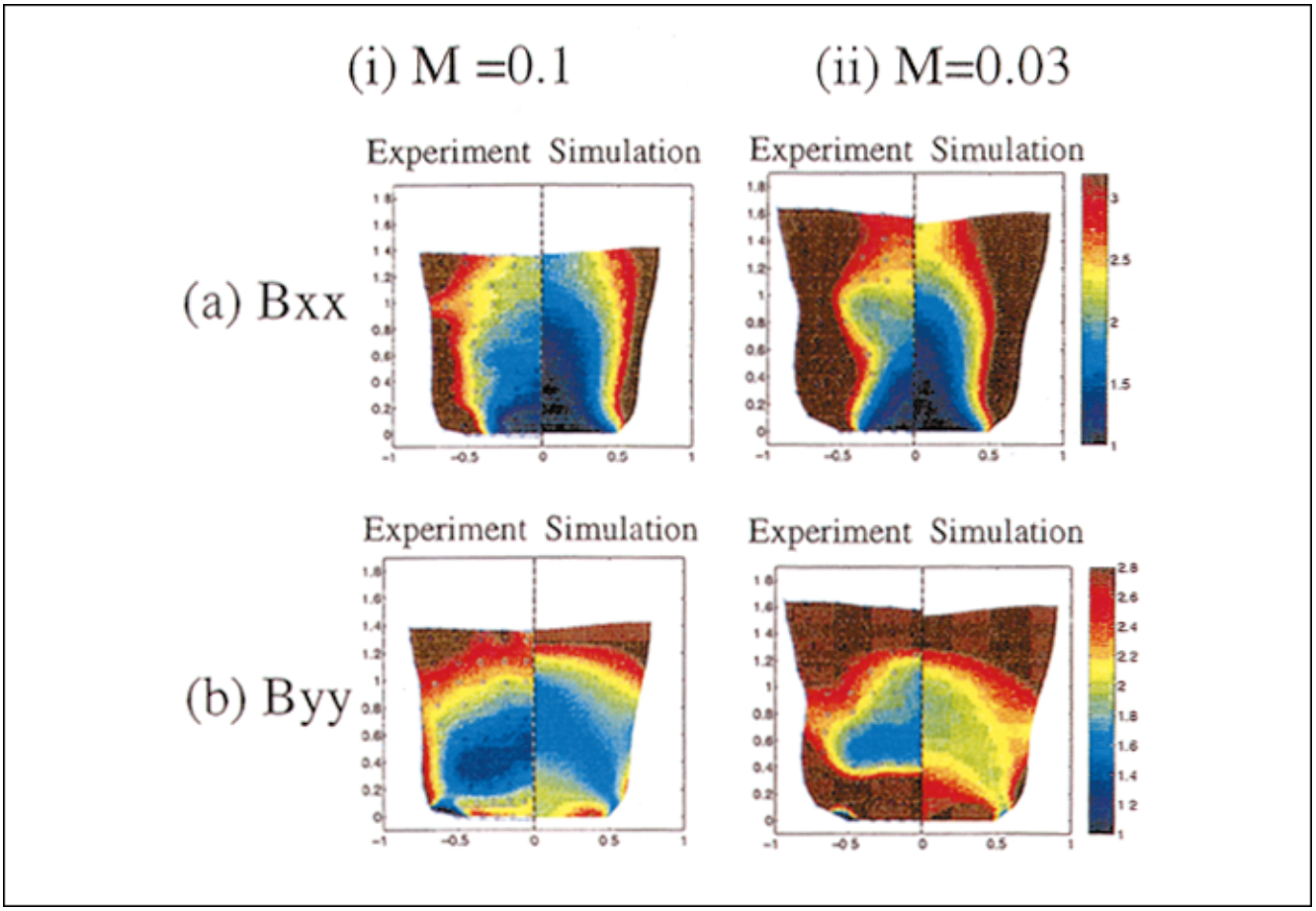

Figure 8. Finger deformation tensor for poly(acrylamide-sodium acrylate) gels after 6 h of swelling in different molarities: 0.1 *M* in (i), and 0.03 *M* in (ii).

B_{xx} and B_{yy} are shown in (a) and (b), respectively. Left experiment; right simulation.

Literature Cited

Achilleos, E. C., R. K. Prudhomme, K. N. Christodoulou, K. R. Gee, and I. G. Kevrekidis, "Dynamic Deformation Visualization in Swelling of Polymer Gels," *Chem. Eng. Sci.*, **55**, 3335 (2000a).

Achilleos, E. C., K. N. Christodoulou, and I. G. Kevrekidis, "A Transport Model for Swelling of Polyelectrolyte Gels in Simple and Complex Geometries," *Comput. Theor. Poly. S.*, in press (2000b).

Anseth, K. S., R. A. Scott, and N. A. Peppas, "Effects of Ionization on the Reaction Behavior and Kinetics of Acrylic Acid Polymerizations," *Macromol.*, **29**, 8308 (1996).

Beck, M., Private communication (1998).

Biage, S. R., M. Harris, W. R. Lempert, and A. J. Smits, "Quantitative Velocity Measurements in Turbulent Taylor-Couette Flow by PHANTOMM Flow Tagging," *Proc. of 8th Int. Symp. on Applications of Laser Techniques in Fluid Mechanics*, Lisbon, Portugal (July 8–11, 1996).

Biorad, *Acrylamide Polymerization— A Practical Approach*, Bulletin 1156, available at http://www.biorad.com/38973.html (last accessed, Feb. 1999).

Buchholz, F. L., and N. A. Peppas, *Superabsorbent Polymers: Science and Technology*, ACS Symp. Series 573, ACS, Washington, DC (1994).

Carmona, R., W. L. Hwang, and B. Torrejani, *Practical Time Frequency Analysis*, 1st ed., Academic Press, San Diego, CA (1998).

Christodoulou, K. N., "Computational Physics of Slide Coating Flow," PhD Diss., University of Minnesota (1990).

Christodoulou, K. N., E. J. Lightfoot, and R. W. Powell, "Stress Induced Defect Formation during Drying of Polymer Films," *AIChE J.*, **44**, 1484 (1998).

Christodoulou, K. N., and L. E. Scriven, "Discretization of Free Surface Flows and Other Moving Boundary Problems," *J. Comp. Phys.*, **99**, 39 (1992).

Curtiss, C. F., and R. B. Bird, "Statistical Mechanics of Transport Phenomena: Polymeric Liquid Mixtures," *Advances in Polymer Science*, J. L. Schrag, ed., Vol. 135, Springer-Verlag, Berlin, p. 1 (1996).

Cussler, E. L., *Diffusion: Mass Transfer in Fluid Systems*, Cambridge University Press, New York (1994).

Dang, W. B., and W. M. Saltzman, "Dextran Retention in the Rat-Brain Following Release from a Polymer Implant," *Biotechnol. Prog.*, **8**, 527 (1992).

Decher, G., and J. D. Hong, "Buildup of Ultrathin Multilayer Films by a Self-Assembly Process. 2. Consecutive Adsorption of Anionic and Cationic Bipolar Amphiphiles and Polyelectrolytes on Charged Surfaces," *Ber. Bunsen. Phys. Chem.*, **95**, 1430 (1991).

Decher, G., J. D. Hong, and J. Schmitt, "Buildup of Ultrathin Multilayer Films by a Self-Assembly Process," *Thin Solid Films*, **210**, 831 (1992).

Doi, M., and A. Onuki, "Dynamic Coupling Between Stress and Composition in Polymer Solutions and Blends," *J. Phys. II France*, **2**, 1631 (1992).

Dubroskii, S. A., M. V. Afanas'eva, N. A. Ryzhkin, and K. S. Kazanskii, "Thermodynamics of Strongly Swollen Polymer Hydrogels," *Poly. Sci. USSR*, **31**, 351 (1989).

Durning, C. J., M. M. Hassan, H. M. Tong, and K. W. Lee, "A Study of Case: II. Transport by Laser Interferometry," *Macromol.*, **28**, 4234 (1995).

Durning, C. J., and K. N. Morman, "Nonlinear Swelling of Polymer Gels," *J. Chem. Phys.*, **98**(5), 4275 (1993).

Edwards, B. J., and A. N. Beris, "Remarks Concerning Compressible Viscoelastic Fluid Models," *JNNFM*, **36**, 411 (1990).

Firestone, B. A., and R. A. Siegel, "Dynamic pH Dependent Swelling Properties of a Hydrophobic Polyelectrolyte Gel," *Poly. Commun.*, **29**, 204 (1988).

Flory, P. J., *Principles of Polymer Chemistry*, Cornell University Press, Ithaca, New York (1953).

Fowler, S. R., and E. A. Guggeheim, *Statistical Thermodynamics*, Cambridge University Press, Cambridge (1965).

Grimshaw, P. E., J. H. Nussbaum, and A. J. Grodzinsky, "Kinetics of Electrically and Chemically Induced Swelling in Polyelectrolyte Gels," *J. Chem. Phys.*, **93**, 4462 (1990).

Haggerty, L., J. H. Sugarman, and R. K. Prud'homme, "Diffusion of Polymers through Polyacrylamide Gels," *Polymer*, **29**, 1058 (1988).

Hariharan, D., and N. A. Peppas, "Modeling of Water Transport in Ionic Hydrophilic Polymers," *J. Polym. Sci., Part B: Polym. Lett.*, **32**, 1093 (1994).

Harmon, J. P., S. Lee, and J. C. M. Li, "Methanol Transport in PMMA: The Effect of Mechanical Deformation," *J. Polym. Sci. Part C*, **25**, 3215 (1987).

Haugland, R. P., *Handbook of Fluorescent Probes and Research Chemicals*, 6th ed., Molecular Probes Inc., Eugene, OR (1996).

Hermans, J. J., "Statistical Thermodynamics of Swollen Polymer Networks," *J. Poly. Sci.*, **59**, 191 (1962).

Hyde, T. M., and L. F. Gladden, "Simultaneous Measurement of Water and Polymer Concentration Profiles during Swelling of Poly(ethylene oxide) using Magnetic Resonance Imaging," *Polymer*, **39**, 811 (1998).

Hyde, T. M., L. F. Gladden, M. R. Mackley, and P. Gao, "Quantitative Nuclear Magnetic Resonance Imaging of Liquids in Swelling Polymers," *J. Poly. Sci. Part A*, **33**(11), 1795 (1995).

Ishihara, A., K. Gee, S. Schwartz, K. Jacobson, and K. Lee, "Photoactivation of Caged Compounds in Single Living Cells: An Application to the Study of Cell Locomotion," *Biotechniques*, **23**, 268 (1997).

Kojima, M., S. Ando, K. Kataoka, T. Hirota, K. Aoyagi, and H. Nakagami, "Magnetic Resonance Imaging (MRI) Study of Swelling and Water Mobility in Micronized Low-Substituted Hydroxypropylcellulose Matrix Tablets," *Chem. Pharm. Bull.* (*Tokyo*), **46**(2), 324 (1998).

Kutter, E. C., K. W. Moser, J. G. Georgiadis, D. Morris, and R. O. Buckius, "Time of Flight vs. Phase Contrast Techniques for MRI Velocimetry," ASME International Mechanical Engineering Congress and Exposition. Symposium on Tomographic Image Reconstruction of Thermal Flows (Nov. 15–20, 1998).

Lempert, W. R., S. Harris, K. Magee, C. L. Burcham, D. Saville, R. B. Miles, K. R. Gee, and R. P. Haugland, "Flow Tagging in Water Using PHoto-Activated Nonintrusive Tracking of Molecular Motion (PHANTOMM), *Proc. Int. Symp. on Appl. of Laser Techniques to Fluid Mechanics*, Lisbon, Portugal (July 11–14, 1994).

Lempert, W. R., K. Magge, P. Ronney, K. R. Gee, and R. P. Haugland, "Flow Tagging Velocimetry in Incompressible Flow Using PHoto-Activated Nonintrusive Tracking of Molecular Motion (PHANTOMM), *Exp. in Fluids*, **18**, 249 (1995).

Lustig, S. R., J. M. Caruthers, and N. A. Peppas, "Continuum Thermodynamics and Transport Theory for Polymer-Fluid Mixtures," *Chem. Eng. Sci.*, **47**, 3037 (1992).

Macosko, C. W., *Rheology: Principles, Measurements, and Applications*, VCH Publishers, Inc., New York (1994).

Mandigo, G., "Imperfections and Heterogeneities in Polyelectrolyte Gels," PhD Diss., Princeton Univ. (1998).

Manning, G. S., "Limiting Laws and Counterion Condensation in Polyelectrolyte Solutions I. Colligative Properties," *J. Chem. Phys.*, **51**, 924 (1969).

Matsuo, E. S., and T. Tanaka, "Kinetics of Discontinuous Volume Phase Transition of Gels," *J. Chem. Phys.*, **89**(3), 1695 (1988).

Mitchison, T. J., K. E. Sawin, and J. A. Therio, "Caged Fluorescent Probes for Monitoring Cytoskeleton Dynamics," *Cell Biology: A Laboratory Handbook*, **3**, 127 (1998).

Moser, K. W., E. C. Kutter, J. G. Georgiadis, and R. O. Buckius, "Velocity Measurements in Pipe with Sudden Contraction and Expansion using Magnetic Resonance Imaging," *Exp. Fluids*, in press (1999).

Onuki, A., "Theory of Phase Transitions in Polymer Gels," *Advances in Polymer Science*, T. Tanaka, ed., Vol. 109, Springer-Verlag, Berlin, p. 63 (1993).

Park, K., *Controlled Drug Delivery*, Amer. Chem. Soc. (1997).

Pettit, D. L., S. S.-H. Wang, K. R. Gee, and G. J. Augustine, "Chemical Two-Photon Uncaging: a Novel Approach to Mapping Glutamate Receptors," *Neuron*, **19**, 465 (1997).

Powell, R. W., K. N. Christodoulou, and I. G. Kevrekidis, "Non-Simple, Multicomponent Mixture Theory for Diffusion of Fluids in Polymers," *Chem. Eng. Sci.*, in review (1999a).

Powell, R. W., K. N. Christodoulou, and I. G. Kevrekidis, "Effect of Network Stress on Solvent Transport in Polymers: a Computer Aided Study in Complex Geometries," *Chem. Eng. Sci.*, in review (1999b).

Sakohara, S., F. Muramoto, and M. Asaeda, "Swelling and Shrinking Processes of Sodium Polyacrylate-Type Super Absorbent Gel in Electrolyte Solutions," *J. Chem. Eng. Jap.*, **23**(2), 119 (1990).

Scherer, G. W., H. Hadach, and J. Phalippou, ''Thermal Expansion of Gels: a Novel Method for Measuring Permeability,'' *J. Non-Cryst. Solids*, **130**, 157 (1991).
Segalman, D. J., and W. R. Witkowski, ''Two-Dimensional Finite Element Analysis of a Polymer Gel Drug Delivery System,'' *Mat. Sci. Eng*., **2**, 243 (1995).
Shahinpoor, M., ''Ionic Polymeric Gels as Artificial Muscles for Robotic and Medical Applications,'' *Iran. J. Sci. Technol.*, **20**, 89 (1996).
Shiga, T., ''Deformation and Viscoelastic Behavior of Polymer Gels in Electric Fields,'' *Adv. Poly. Sci*., **134**, 131 (1997).
Siegel, R. A., M. Falamarzian, B. A. Firestone, and B. C. Moxley, ''pH-Controlled Release from Hydrophobic/Polyelectrolyte Copolymer Hydrogels,'' *J. Controlled Release*, **8**, 179 (1988).
Smith, K. J., A. Ciferri, and J. J. Hermans, ''Anisotropic Elasticity of Composite Molecular Networks Formed from Non-Gaussian Chains,'' *J. Poly. Sci. Part A*, **2**, 1025 (1964).
Stigter, D., ''The Charged Colloidal Cylinder with a Gouy Double Layer,'' *J. Coll. Int. Sci*., **53**(2), 296 (1975).
Tanaka, T., ''Dynamics of Critical Concentration Fluctuations in Gels,'' *Phys. Rev. A*, **17**, 763 (1978).
Tanaka, T., and D. Fillmore, ''Kinetics of Swelling of Gels,'' *J. Chem. Phys*., **70**, 1214 (1979).
Tanaka, T., L. O. Hocker, and G. B. Benedek, ''Spectrum of Light Scattered from a Viscoelastic Gel,'' *J. Chem. Phys*., **59**, 5151 (1973).
Tokita, M., ''Friction between Polymer Networks of Gels and Solvent,'' *Adv. Poly. Sci*., **110**, 27 (1993).
Tong, J., ''Partitioning and Diffusion of Macromolecules in Polyacrylamide Gels,'' PhD Diss., Carnegie Mellon Univ., Pittsburgh, PA (1995).
Tong, J., and J. L. Anderson, ''Partitioning and Diffusion of Proteins and Linear Polymer in Polyacrylamide Gels,'' *Biophys. J*., **70**, 1505 (1996).
Wang, C. J., Y. Li, and Z. B. Hu, ''Swelling Kinetics of Polymer Gels,'' *Macromol*., **30**, 4727 (1997).
Yin, Y., ''Swelling Behavior of Polyelectrolyte Gels,'' PhD Diss., Princeton Univ. (1993).
Yin, Y. L., R. K. Prud'homme, and F. Stanley, ''Relationship between Poly(acrylic acid) Gel Structure and Synthesis,'' A. J. Harland and R. K. Prud'homme, eds., *Polyelectrolyte Gels*, ACS Symp. Ser. 480 (1992).

Manuscript received Apr. 9, 1999, and revision received May 23, 2000.